Soft Matter

www.rsc.org/softmatter

Volume 8 | Number 30 | 14 August 2012 | Pages 7729–7990

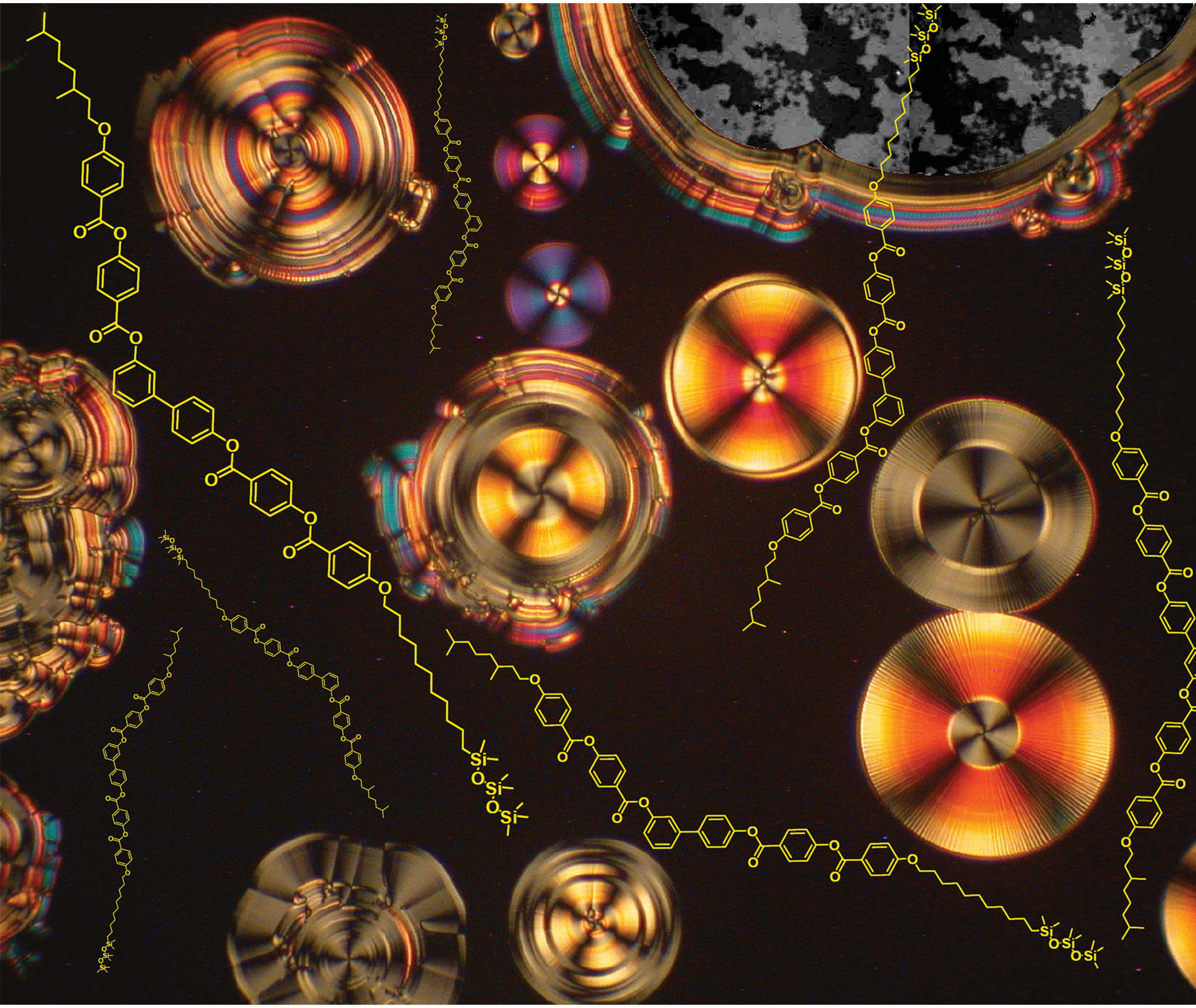

ISSN 1744-683X

RSC Publishing

PAPER
Hale Ocak *et al.*
Effects of molecular chirality on superstructural chirality in liquid crystalline dark conglomerate phases

1744-683X(2012)8:30;1-B

Soft Matter

Dynamic Article Links

Cite this: *Soft Matter*, 2012, **8**, 7773

www.rsc.org/softmatter

PAPER

Effects of molecular chirality on superstructural chirality in liquid crystalline dark conglomerate phases†

Hale Ocak,*[a] Belkız Bilgin-Eran,[a] Marko Prehm[bc] and Carsten Tschierske*[c]

Received 1st April 2012, Accepted 1st May 2012
DOI: 10.1039/c2sm25763g

The first examples of polyphilic bent-core compounds consisting of a biphenyl central core, a chiral terminal chain and an oligo(dimethylsiloxane) end group at the other terminus have been synthesized and characterized. The mesomorphic behaviour of the compounds was investigated by differential scanning calorimetry, optical polarizing microscopy, X-ray diffraction and electro-optic methods. The olefinic precursors show monotropic or enantiotropic B_1 type mesophases. The siloxane substituted analogues containing a racemic chain exhibit dark conglomerate phases ($DC^{[*]}$ phases) which are composed of chiral domains with opposite chirality, whereas the siloxane derivatives with a homogeneously chiral moiety show "dark enantiomer" phases (DE* phases) with uniform chirality. Under electric fields, different types of ferroelectric switching (FE) smectic and modulated smectic phases were induced. The effects of chain branching, spacer length and molecular chirality on the stability of the $DC_{FE}^{[*]}$ and DE_{FE}^{*} phases and on the field-induced smectic and modulated smectic phases were investigated.

1. Introduction

Spontaneous achiral symmetry breaking, *i.e.* the spontaneous formation of chiral superstructures with uniform chirality over macroscopic dimensions, achieved by self-assembly of achiral or racemic molecules, has been a core research topic since it was discovered by Pasteur.[1,2] Recently, work on the phenomenon of spontaneous reflection symmetry breaking in supramolecular ensembles[3–5] has moved into fluid liquid crystalline (LC) phases,[6–12] namely LC phases formed by bent-core molecules.[13–19] Superstructural chirality in the LC phases of these materials result from the polar order in their lamellar (smectic) LC phases ($SmCP_A$, $SmCP_F$, see Fig. 1a).[13,15] The combination of tilt and polar order leads to an intrinsic chirality of the layers formed by these achiral molecules (Fig. 1b).[13,15]

Chirality in LC phases, either molecular or superstructural in origin, leads to chirality-modified and chirality-frustrated LC phases and ferroelectricity.[16,20–23] Though few bent-core molecules containing chiral centers in the terminal chains have been reported so far,[24–32] and diastereomeric relations between layer chirality and molecular chirality have recently been observed in switching experiments,[32] the effects of the combination of molecular chirality with superstructural chirality in LC phases of bent-core molecules are only partially explored to date.

For this reason, we have synthesized and investigated chiral polyphilic bent-core mesogens. The introduction of polyphilicity[33] into bent-core LC molecules has been used to stabilize smectic phases and to modify the interlayer correlations. In particular, oligo(dimethylsiloxane) units represent useful structural units capable of segregation into their own domains (Fig. 1c).[13a,34–39] Attached to bent-core units, these moieties lead to ferroelectric switching LC phases ($SmCP_F$)[34] instead of the usually observed antiferroelectric phases ($SmCP_A$), and often the so-called "dark conglomerate phases" ($DC^{[*]}$ phases) can be observed.[34,40–45] In these non-birefringent or low-birefringent mesophases, which appear dark between crossed polarizers, macroscopic chirality can be identified by the occurrence of a conglomerate of chiral domains with opposite handedness.[13a,34,38,39] The low birefringence of these mesophases is thought to result from an intrinsic layer frustration due to the packing of the bent-cores in a flat layer, leading to a saddle splay deformation. In this way the 3-dimensionally deformed layers become organized in a sponge-like super-structure (Fig. 1d).[46] Due to this special spatial organization of the layers, these LC phases appear optically isotropic. In these soft matter systems the layer chirality couples with the molecular conformational chirality that provides significant optical activity.[13a,47,48] Because there is no birefringence in these DC phases, chirality can easily be detected by optical investigations.

---

[a] *Department of Chemistry, Yildiz Technical University, Davutpaşa Yerleşim Birimi, TR-34210 Esenler Istanbul, Turkey. E-mail: ocak_hale@hotmail.com*
[b] *Institute of Chemistry, Physical Chemistry, Martin Luther University Halle-Wittenberg, Von-Danckelmann-Platz 4, D-06120 Halle, Germany*
[c] *Institute of Chemistry, Organic Chemistry, Martin Luther University Halle-Wittenberg, Kurt Mothes-Str. 2, D-06120 Halle, Germany. E-mail: carsten.tschierske@chemie.uni-halle.de*

† Electronic supplementary information (ESI) available. See DOI: 10.1039/c2sm25763g

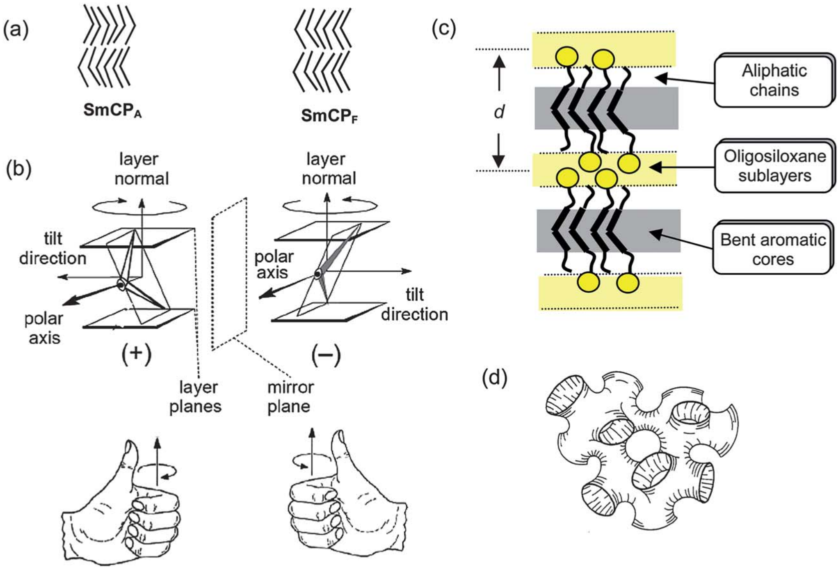

Fig. 1 The fundamental modes of molecular organization in the polar smectic phases of bent-core mesogens: (a) ferroelectric and antiferroelectric polar order in tilted smectic (SmCP$_{A/F}$) phases (the tilt occurs perpendicular to the bend directions), (b) superstructural chirality arising from the combination of tilt and polar order, (c) formation of triply segregated layers by polyphilic bent-core mesogens with terminal silyl groups and (d) sponge-like deformation of the layers in the dark conglomerate phases.[13a,16,39a,d]

Herein, we present the first examples of bent-core mesogens combining chiral chains with siloxane units, known to force the formation of dark conglomerate phases, thereby combining the effects of molecular chirality with superstructural chirality. The influence of the branched chiral chains on the self-assembly of siloxane substituted bent-core molecules is studied and the enantiomers are compared with the racemic mixtures.

2. Results and discussion

2.1 Synthesis

The bent-core compounds **1–3** with terminal double bonds were synthesized as shown in Scheme 1 by stepwise esterification[49] of 4′-benzyloxybiphenyl-3-ol (**A**),[50] using *N*,*N*′-dicyclohexylcarbodiimide (DCC) at first with chiral 4-(4-alkyloxybenzoyloxy)benzoic acids (**B**),[32,51] followed by hydrogenolytic debenzylation (H_2, Pd/C in THF)[39a] and DCC esterification[49] of the biphenylols **C** with the appropriate 4-[4-(alkenyloxy)-benzoyloxy]benzoic acids (**D/*n***)[52,53] according to known procedures.[37,39a,c] The chiral alkyloxy groups of the benzoic acids **B** were introduced by an etherification reaction of ethyl 4-hydroxybenzoate with the appropriate tosylates which were prepared from the corresponding commercially available chiral alcohols by tosylation.[54] After hydrolysis, the chiral 4-alkyloxybenzoic acids were used for DCC esterification with 4-hydroxybenzaldehyde. The resulting 4-(4-alkyloxybenzoyloxy) benzaldehydes were oxidized using sodium chlorite as the oxidizing agent to yield the acids **B**.[52] For the synthesis of compound **(*S*)-3b**, (*S*)-(−)-β-citronellol was used as the starting material and the double bond was hydrogenated to the (*S*)-3,7-dimethyloctyloxy unit during the hydrogenolytic deprotection of the benzyl group. In the final step 1*H*-heptamethyltrisiloxane **H–Si$_3$** or 3*H*-heptamethyltrisiloxane **H–Si$_{3i}$**, respectively, were attached to the olefins **1–3** by a hydrosilylation reaction[39a,55] using Karstedt's catalyst to yield the siloxanes **Si$_x$-1** to **Si$_x$-3**. From the synthetic procedure it is clear that the stereogenic centers of the starting alcohols were not touched and hence, it can be assumed that the final products have equal optical purity to the used starting material. Purification of all final compounds was carried out by column chromatography on silica gel and crystallization from ethanol. The experimental details, spectroscopic (^{1}H-NMR, ^{13}C-NMR and MS) and analytic data of the materials are given in the ESI†.

2.2 Investigation of the liquid crystalline properties

The mesomorphic properties of the synthesized olefins **1–3** and silylated compounds **Si$_x$-1**–**Si$_x$-3** were investigated by polarised light optical microscopy (PM), differential scanning calorimetry (DSC), and electro-optical measurement, some of them also by X-ray diffraction (XRD).

2.3 Mesophases of the olefins 1–3

All compounds combining an olefinic group at one end and a branched chain at the other exhibit monotropic or enantiotropic B$_1$ mesophases (Table 1), as indicated by the XRD of the aligned samples. The small angle diffraction pattern of the B$_1$ phase of compound **(*S*)-1a** can be indexed to a rectangular lattice (*c*2*mm*) with the lattice parameters $a = 2.6$ nm and $b = 4.1$ nm (at 150 °C, see Fig. 2a and b). The diffuse wide angle scattering is perpendicular to *b*, which means that the molecules are aligned parallel to *b* and *a*/2 corresponds to the diameter of the ribbon forming the rectangular lattice (Fig. 2c). The parameter *b* is in good agreement with the molecular length ($L_{mol} = 4.3$ nm for 120° bent molecules with the most stretched wing groups determined by space filling molecular models) and the number of molecules arranged in the cross-section of the ribbons is about only three. Slightly larger ribbons comprising about 5 molecules

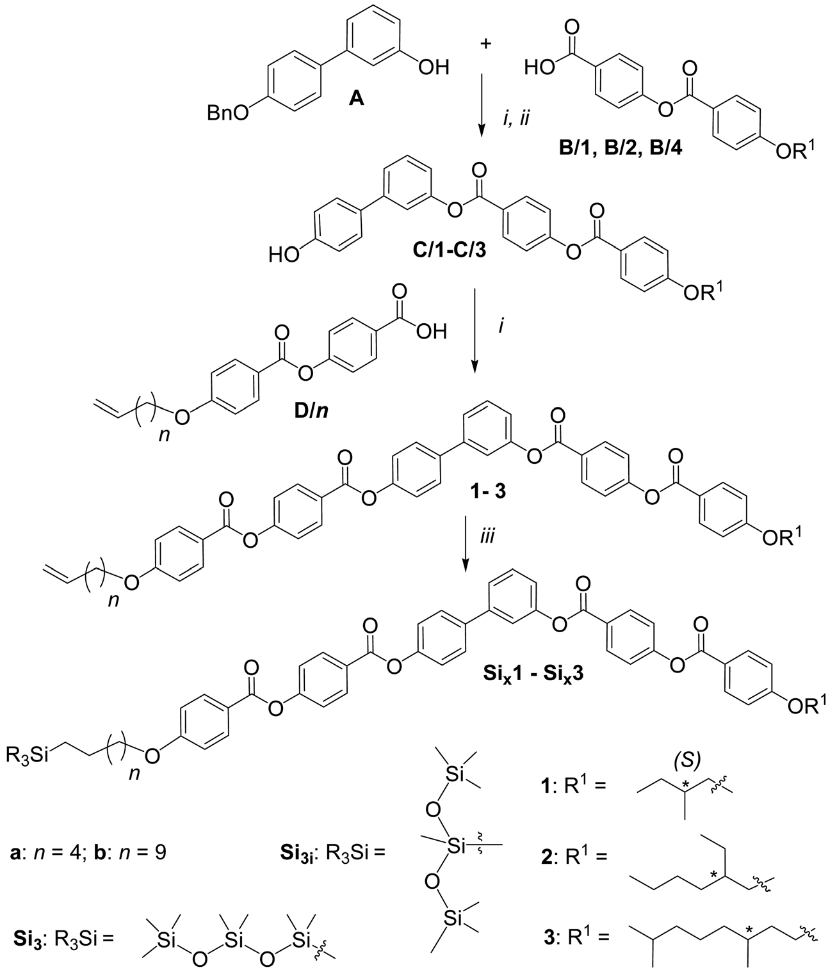

Scheme 1 Synthesis of the chiral oligo(dimethylsiloxane) substituted bent-core compounds. *Reagents and conditions*: (i) DCC, DMAP, CH_2Cl_2, r.t.;[49] (ii) H_2, Pd/C, THF, 40 °C, 18 h;[39a] (iii) **H–Si$_x$**, Karstedt's catalyst, toluene, r.t., 48 h;[39a,55] for preparation of **C/3** the benzoic acid **B/4** with R^1 = (*S*)-(−)-β-citronellyl is used; the double bond is hydrogenated in step (ii).

organized side-by-side (a = 3.7 nm, b = 4.8 nm at 110 °C) were observed for the B_1 phase of ***rac*-3b** (see Fig. S1†). Surprisingly, the fan-like texture of the mesophase of compound **(*S*)-1a** (Fig. 3a) is more similar to a B_6-type intercalated smectic phase, whereas for all other synthesized compounds the typical textures of B_1 phases (Fig. 3b) were observed. This is in line with the model of the B_1 phases, which are related to the B_6 phases, mainly differing in the correlation length of the two-dimensional (2d) lattice, which is long range for the B_1 phases and only short range for the B_6 phases.[56] Compound **(*S*)-1a** appears to be an intermediate case showing a B_6-like fan-texture though a 2d lattice is already observable by XRD. No polar switching could be observed for these mesophases in the electro-optical studies, which is also in line with other B_1 phases.[13]

As shown in Table 1, the stability of the B_1 phases decreases with growing effective diameter of the branched chain (2-methylbutyl > 3,7-dimethyloctyl > 2-ethylhexyl), determined by the position of the chain branching and the length of the branch located closest to the core. Stability is also affected by the alkenyl chain length and decreases in the order n = 4 (**a**) > n = 9 (**b**).

Comparing the mesomorphic properties of the enantiomer **(*S*)-3b** with the racemic compound ***rac*-3b** shows that the mesophase stability and mesophase type remain the same, indicating the absence of a significant chirality effect on the formation of the B_1 phases.[28]

2.4 Mesophases of the siloxanes

The phase transition temperatures of the silylated compounds **Si$_x$-1–Si$_x$-3** are collated in Table 2. All compounds exhibit mesophases which appear dark (optically isotropic) between crossed polarizers, but for some racemic compounds (compounds ***rac*-Si$_3$-3a** and ***rac*-Si$_{3i}$-3b**) small birefringent defects can be observed. The transition from the isotropic liquid state to these dark mesophases is indicated in the DSC scans by relatively high transition enthalpy values between 15 and 21 kJ mol^{-1} as typical for the transition to polar mesophases for bent-core molecules.[13] Optically there is no change, only a strong increase of the viscosity is observed at these temperatures. On further cooling the viscosity increases further at temperatures between 70 and 85 °C, but the dark appearance of the mesophase does not change and no peak or distinct step is observed in the DSC curves (see Fig. 4 for an example). However, in the heating curves a small hump starts around this temperature. It appears that at

Table 1 Mesophases, phase transition temperatures and transition enthalpies of the olefins **1–3**[a]

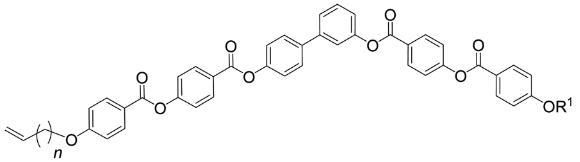

Compound	*n*	R^1	T/°C [ΔH/kJ mol^{-1}]
(*S*)-1a	4	(*S*)-2-Methylbutyl	Cr 143 [22.3] B_1 166 [11.1] Iso
***rac*-2a**	4	*rac*-2-Ethylhexyl	Cr 125 [35.7] (B_1 108 [6.4]) Iso
***rac*-2b**	9	*rac*-2-Ethylhexyl	Cr 111 [22.9] (B_1 99 [4.0]) Iso
***rac*-3a**	4	*rac*-3,7-Dimethyloctyl	Cr_1 80 [8.9] Cr_2 104 [4.6] B_1 139 [9.2] Iso
***rac*-3b**	9	*rac*-3,7-Dimethyloctyl	Cr 105 [33.3] B_1 123 [12.8] Iso
(*S*)-3b	9	(*S*)-3,7-Dimethyloctyl	Cr 61 [4.1][b] B_1 124 [11.7] Iso

[a] Perkin-Elmer DSC-7; peak temperatures of the first heating scans at a rate of 10 K min^{-1}; enthalpy values are given in square parentheses; abbreviations: Cr = crystalline; B_1 = rectangular columnar phase with a *c2mm* lattice, the molecules are non-tilted and the polarization is antiparallel and along the column long axes ($B_{1\text{rev}}$ phases, see model in Fig. 2c) and Iso = isotropic liquid phase; monotropic transitions are indicated by parentheses. [b] Partial crystallization.

this temperature the mesophase enters into a kind of glassy state.[39d] With the exception of compound **(*S*)-Si$_3$-1a**, apparently none of the compounds crystallize.

2.4.1 Optical investigations.

For the racemic compounds ***rac*-Si$_3$-2a** and ***rac*-Si$_x$-3a/b** a mixture of dark and bright domains become visible by rotating the polarizer by a small angle (2–3°) either clockwise or anti clockwise. If the polarizer is rotated in the opposite direction, the brightness of the domains is reversed as shown in Fig. 5a and c. No domains were observed if the sample was rotated between the crossed polarizers and the brightness of the chiral domains was not changed if the sample was rotated between slightly decrossed polarizers. This indicates a conglomerate of domains with opposite chirality as typical for dark conglomerate (DC[*]) phases.[34,35,39] For the racemic compounds ***rac*-Si$_x$-2b** no chiral domains can be detected and the brightness increases equally by decrossing the polarizers in either direction. For these compounds the chiral domains are either too small to be detected by optical microscopy or the phase itself is achiral if layers with opposite chirality alternate.[57] Based on electro-optical investigations (see below) it appears that the sponge-like layer deformation is especially strong for these compounds and hence it is likely that also the chiral domains are indeed much smaller than in other cases. Therefore these mesophases are assigned as DC phases (without [*]) here.

The mesophases of the enantiomers **(*S*)-Si$_3$-1a** and **(*S*)-Si$_3$-3b** also appear optically isotropic between crossed polarizers and no chiral domains could be observed by decrossing the polarizers Fig. 5d–f. However, for these compounds the brightness depends on the direction of inclination of the polarizers with respect to the 90° position. A comparison of the mesophase stability of the compounds ***rac*-Si$_3$-3b** and **(*S*)-Si$_3$-3b** shows that the phase transition temperatures remain the same by replacing the racemic chain by a homogeneously chiral chain. From contact preparations between the enantiomer **(*S*)-Si$_3$-3b** and the related racemic compound ***rac*-Si$_3$-3b** it is evident that the chirality sense of the domains is biased by the molecular chirality (see Fig. 5g and h). Only one type of chiral domain is formed by the enantiomerically pure compound (dark enantiomer phases, DE* phases), whereas the racemic compound shows domains with opposite chirality in the ratio 1 : 1 (DC[*] phases). In the contact region between the racemic mixture and the enantiomer the dominance of one type of domain at first increases and then the other type of domain is completely removed. Though it was shown previously that chiral additives can change the dark conglomerate phases to a uniformly chiral texture,[42] to the best of our knowledge the

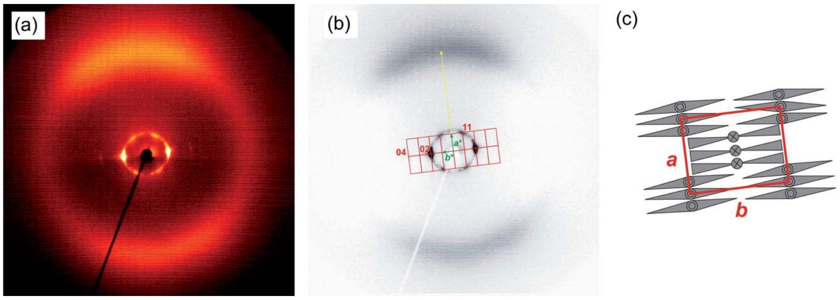

Fig. 2 X-ray diffraction patterns of compound **(*S*)-1a** in the B_1 mesophase (a = 2.6 nm; b = 4.1 nm) at T = 150 °C; (a) original wide angle pattern; (b) the same pattern after subtraction of the scattering in the isotropic liquid state with the reciprocal lattice and indexation and (c) model of the molecular organization in the B_1 phase.

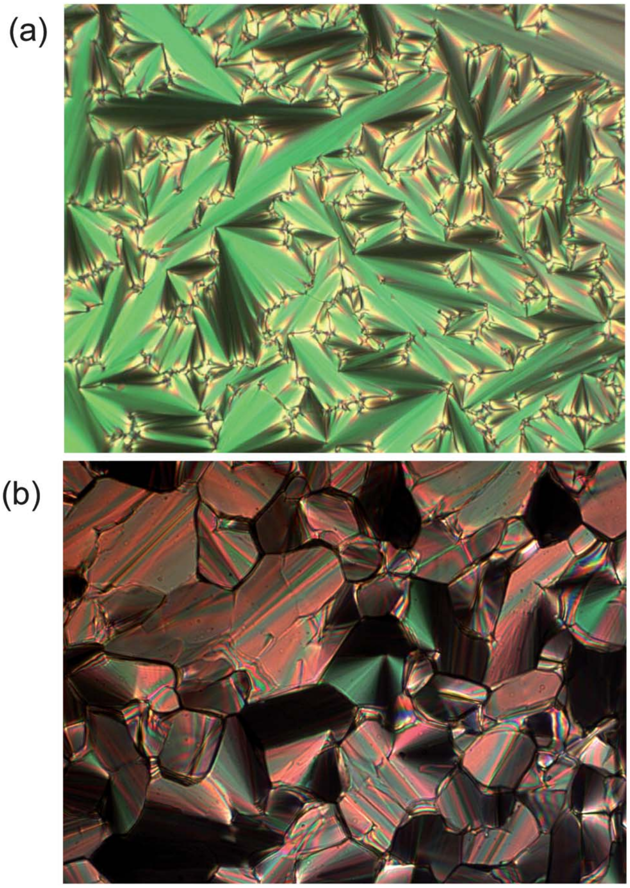

Fig. 3 The textures obtained between crossed polarizers as observed for the B$_1$ phases of (a) **(_S_)-1a** at 156 °C and (b) **_rac_-3b** at 116 °C.

compounds reported here represent the first dark phases formed by chiral bent-core LC molecules. As these mesophases are uniformly chiral and do not represent conglomerates they are assigned as "dark enantiomer phases" (DE* phases) in analogy to the DC$^{[*]}$ phases formed by the racemates. The textural features are dark (optically isotropic) uniform textures, where the maximum darkness is achieved by slightly decrossing the polarizers in a specific direction (clockwise or counterclockwise). The maximum contrast is obtained for approximately the same angles as observed for the DC$^{[*]}$ phases (2–3°) of the corresponding racemate, suggesting that it is mainly determined by the chiral superstructure than by the molecular chirality. Therefore, the major effect of molecular configurational chirality seems to be the bias of the conformational chirality of the molecules.

Though the DE* phases of the investigated enantiomerically pure compounds always appear uniformly dark without birefringent defects, for the DC$^{[*]}$ phases of the racemic compounds in some cases small birefringent defects were observed, especially for compounds **_rac_-Si$_3$-3a** and **_rac_-Si$_{3i}$-3b**. This might be due to some distortion of the sponge-like structure. The racemic compounds seem to be more sensitive to this kind of distortion, probably due to the presence of the conglomerate structure with grain boundaries between domains with opposite chirality. These boundaries might induce some distortion to the sponge-like structure, *i.e.* there are regions with a not completely random and locally lamellar structure that appear birefringent.

2.4.2 XRD investigations. In the XRD patterns of the mesophase of the compound **_rac_-Si$_3$-2a**, shown in Fig. 6, there are two diffuse scatterings in the wide-angle region. One has a maximum at $d = 0.47$ nm, corresponding to the mean distance between the aromatic cores and the alkyl chains and a second one, which is much weaker and has its maximum at $d = 0.70$ nm. It is assigned to the mean distance between the segregated oligo(dimethylsiloxane) units.[39a,c] One intense reflection is observed in the small angle region together with very weak 2nd and 3rd order reflections as typical for lamellar phases. The *d*-value is smaller than the molecular length and would be in line with a tilted organization of the molecules in layers. It is now accepted that DC$^{[*]}$ phases represent smectic phases with sponge-like deformed layers.[46] For this reason uniform alignment of the samples is impossible and therefore only a ring with uniform brightness is observed for the layer reflection in the XRD patterns (after attempted surface alignment). This kind of diffraction pattern is very typical for DC$^{[*]}$ phases[39a] (for additional diffraction patterns, see Fig. S2–S4†), but it prevents the precise determination of the phase structure by 2d-XRD. If a sponge-like structure formed by lamellae is assumed, then from the *d*-values ($d = 3.8$ nm for **rac-Si$_3$-2a** at 110 °C and $d = 4.5$ nm for compound **_rac_-Si$_3$-3b** at 100 °C (Fig. S2†)) tilt angles around 50° and 42°, respectively, can be estimated according to $\cos\beta = d/L_{\mathrm{mol}}$ (**_rac_-Si$_3$-2a**: $L_{\mathrm{mol}} = 5.9$ nm; **_rac_-Si$_3$-3b**: $L_{\mathrm{mol}} = 6.1$ nm). Such high tilt angles between 35° and 50° are reasonable values for SmCP phases formed by bent-core mesogens.[13]

In the temperature range between 70 and 80 °C the small angle scattering becomes more diffuse and the viscosity increases. This supports the idea of a transition to a glassy state at this temperature.[39d]

2.4.3 Electro-optical investigation of the siloxanes *rac*-Si$_x$-3.

Electro-optical investigations were carried out in 6 μm indium tin oxide (ITO) coated cells without additional polyimide (PI) alignment layer. The textural changes observed under the electric field and the type of response on an applied triangular wave field strongly depend on the molecular structure, applied voltage and temperature.

The dark conglomerate phases of the racemic compounds **_rac_-Si$_{3i}$-3b** and **_rac_-Si$_3$-3a** become strongly birefringent under an applied electric field of 22 V μm^{-1} and 26 V μm^{-1}, respectively. These threshold fields are required for the removal of layer deformation and induction of strongly birefringent smectic phases, which are then further stabilized by surface interaction (Fig. 7b).[13a] These field-induced smectic phases show only one very sharp current peak in the half period of a triangular wave voltage, indicating a ferroelectric switching process. The position of the peak maximum is at relatively low voltage (2 V μm^{-1} and 3 V μm^{-1}, respectively, see Fig. 7a and c) but at slightly higher voltage compared to related silylated bent-core mesogens with linear alkyl chains ($\ll$1 V μm^{-1}).[39a] The calculated polarization values are 570 and 680 nC cm^{-2} and these values are in the typical range observed for polar SmCP phases of bent-core mesogens.[39a] However, it seems that the field-induced smectic layers still retain some layer undulation or layer modulation, as indicated by the distinct textures (Fig. 7b and d) and by the position of the current peak maxima at increased voltage. For this reason these dark conglomerate phases, showing ferroelectric switching, are

Table 2 Mesophases, phase transitions, transition enthalpies and spontaneous polarization values (P_s) of the silylated compounds **Si$_x$-1–Si$_x$-3**[a]

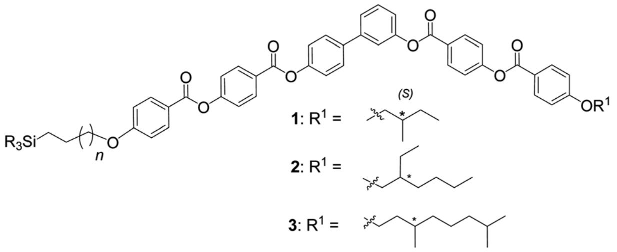

Compound	R$_3$Si–	n	R^1	T/°C [ΔH/kJ mol^{-1}]	P_s/nC cm^{-2} (T/°C)
(*S*)-Si$_3$-1a	Me$_3$Si(OMe$_2$Si)$_2$–	4	(*S*)-1	Cr$_1$ 123 [10.4] Cr$_2$ 142 [13.6] Iso Iso 140 [18.7] DE$_{FE}$* 75 DE$_{(g)}$*	330 (114)
***rac*-Si$_3$-2a**	Me$_3$Si(OMe$_2$Si)$_2$–	4	*rac*-2	DC$_{FE}$$^{[*]}$ 119 [16.9] Iso Iso 116 [17.1] DC$_{FE}$$^{[*]}$ 85 DC$_{(g)}$$^{[*]}$	3.5 (108)
***rac*-Si$_{3i}$-2b**	(Me$_3$SiO)$_2$MeSi–	9	*rac*-2	DC 126 [17.8] Iso Iso 126 [17.6] DC 70 DC$_{(g)}$	—
***rac*-Si$_3$-2b**	Me$_3$Si(OMe$_2$Si)$_2$–	9	*rac*-2	DC127 [17.8] Iso Iso 125 [17.5] DC 70 DC$_{(g)}$	—
***rac*-Si$_3$-3a**	Me$_3$Si(OMe$_2$Si)$_2$–	4	*rac*-3	DC$_{FE}$$^{[*]}$ 140 [14.6] Iso Iso 141 [15.0] DC$_{FE}$$^{[*]}$ 72 DC$_{(g)}$$^{[*]}$	680 (131)
***rac*-Si$_{3i}$-3b**	(Me$_3$SiO)$_2$MeSi–	9	*rac*-3	DC$_{FE}$$^{[*]}$ 150 [18.2] Iso Iso 146 [17.3] DC$_{FE}$$^{[*]}$ 70 DC$_{(g)}$$^{[*]}$	570 (136)
***rac*-Si$_3$-3b**	Me$_3$Si(OMe$_2$Si)$_2$–	9	*rac*-3	DC$_{FE}$$^{[*]}$ 149 [20.7] Iso Iso 148 [20.5] DC$_{FE}$$^{[*]}$ 75 DC$_{(g)}$$^{[*]}$	720 (120)
(*S*)-Si$_3$-3b	Me$_3$Si(OMe$_2$Si)$_2$–	9	(*S*)-3	DE$_{FE}$* 152 [19.9] Iso Iso 149 [19.9] DE$_{FE}$* 75 DE$_{(g)}$*	650 (120)

[a] Perkin-Elmer DSC-7; heating (top lines)/cooling (bottom lines) rates were 10 K min^{-1}; enthalpy values are given in square parentheses; abbreviations: DC$_{FE}$$^{[*]}$ = dark conglomerate phase showing ferroelectric switching, DE$_{FE}$* = dark mesophase with uniform chirality sense showing ferroelectric switching; DC = non-switching dark mesophase without visible chiral domains; DC$_{(g)}$$^{[*]}$, DE$_{(g)}$* and DC$_{(g)}$ indicate the non-switching glassy states of the DC$_{FE}$$^{[*]}$, DE$_{FE}$* and DC phases, respectively.

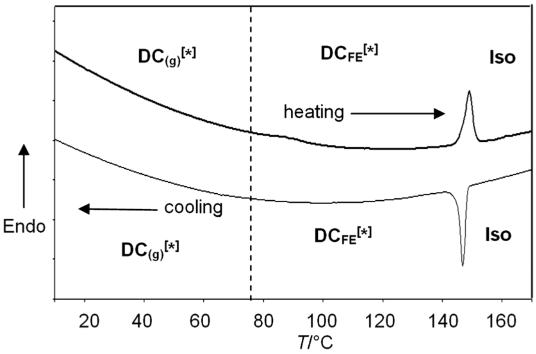

Fig. 4 DSC heating and cooling curve of compound ***rac*-Si$_3$-3b** (10 K min^{-1}).

assigned as DC$_{FE}$$^{[*]}$ phases instead of SmCP$_{FE}$$^{[*]}$, which was used previously for DC$^{[*]}$ phases forming non-modulated field-induced smectic phases.[13a,34a,39] Below about 75 °C, when the viscosity of the mesophase increases, the switching peak disappears completely, which is in line with the proposed glass transition at this temperature (DC$_{(g)}$$^{[*]}$ phase).[39d]

2.4.4 Comparative electro-optical investigation of racemic compounds and enantiomers. In order to study the effect of chirality on the electro-optical behaviour, the racemic compound ***rac*-Si$_3$-3b** and the corresponding enantiomer **(*S*)-Si$_3$-3b** have been investigated and compared. Both compounds exhibit a sharp single polarization current peak per half period of the applied triangular wave voltage (see Fig. 8 and 9) with high values of the spontaneous polarization of 720 and 650 nC cm^{-2}, respectively. However, the textures observed for the field-induced states at identical field strength (6 V μm^{-1}) are different for the racemic compound and the enantiomer.

The birefringence of the texture of the racemic compound ***rac*-Si$_3$-3b** in the field-induced state (see Fig. 8b and d) is lower than that observed for the enantiomer **(*S*)-Si$_3$-3b** (Fig. 9b and d) which indicates an increased stability of the sponge-like DC$^{[*]}$ structure of the racemic compound with respect to distortion by external electric fields. Reducing the temperature increases the contribution of birefringent areas (see Fig. 8b and d) and as the birefringence increases the polarization peak grows (Fig. 8a and c). Because the current peak occurs at relatively high voltage (*ca.* 4–5 V μm^{-1}, see Fig. 8a and c) it is likely that in the birefringent texture significant layer modulation is retained.

The field-induced texture of the enantiomer **(*S*)-Si$_3$-3b** (Fig. 9b) has a much higher birefringence, indicating that the sponge-like layer deformation is completely removed in this case. However, the texture is untypical for a smectic phase, but appears more similar to the textures of modulated smectic phases. This means that in the chiral compound the sponge structure is much more easily removed, but layer distortion is retained, leading to a modulated smectic phase. Also the position of the current peak at relatively high voltage (4 V μm^{-1}) is in line with

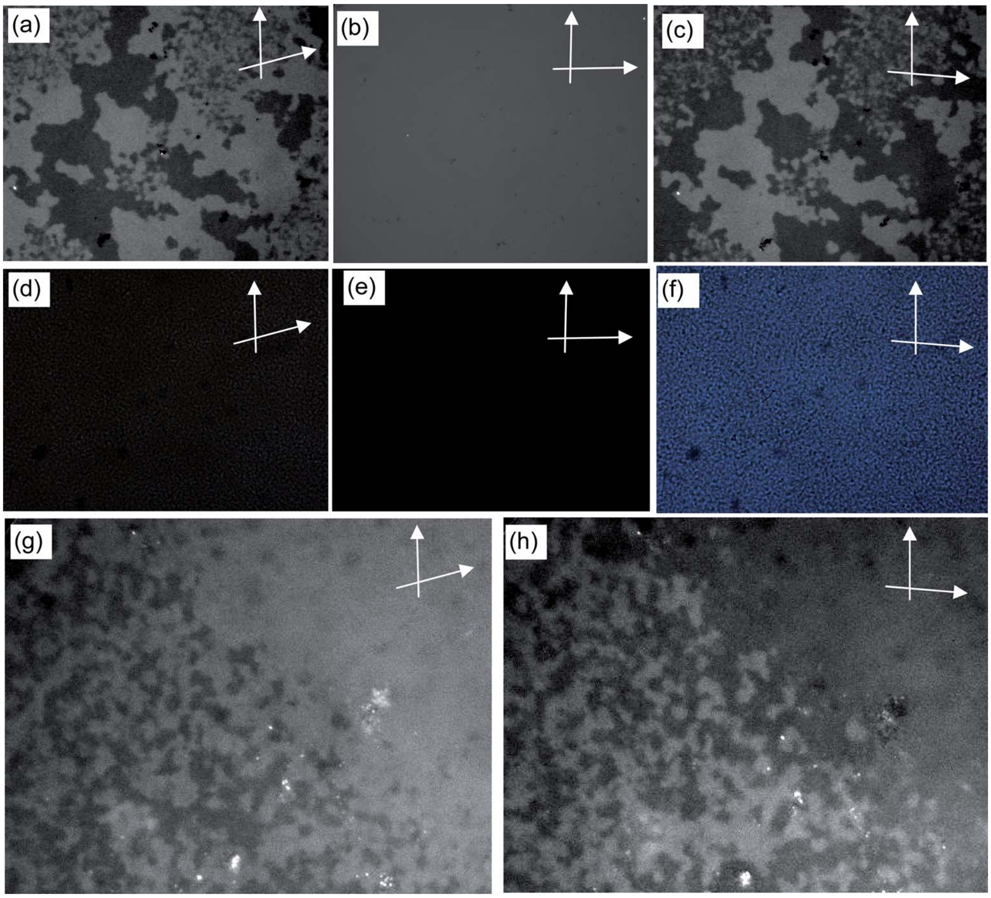

Fig. 5 Comparison of the textures of $DC^{[*]}$ and DE* phases between crossed polarizers and after decrossing the polarizers. (a–c) The chiral domains of ***rac*-Si$_3$-3b** in the $DC_{FE}{}^{[*]}$ phase at 130 °C; (a and c) between slightly uncrossed polarizers (±10°) (b) between crossed polarizers; (d–f) the homogeneously chiral DE* phase of the **(*S*)-Si$_3$-1a** phase at 137 °C; (d and f) between slightly uncrossed polarizers (±3°) and (e) between crossed polarizers; (g and h) the contact region between the $DC_{FE}{}^{[*]}$ phase of the ***rac*-Si$_3$-3b** (bottom left) and the DE_{FE}* phase of the **(*S*)-Si$_3$-3b** (top right) at 132 °C between uncrossed polarizers (±10°). The contrast in (a–c) and (g and h) was increased to improve visibility of the domains.

the presence of significant layer modulation. Only after applying a much higher voltage the texture becomes more fan-like (Fig. 9d). In addition, a polarization current peak close to 0 V crossing (<1 V μm^{-1}), as typical for non-distorted SmCP$_F$ states, is observed beside the residual peak at significantly higher voltage (4 V μm^{-1}), assigned to the switching of the remaining modulated smectic phase (Fig. 9a and c). The coexistence of modulated and non-modulated (or weakly modulated) field-induced smectic states might be due to surface interactions, which change their influence depending on the distance to the surfaces.

These investigations provide some evidence that the sponge-like deformation of the layers is more stable in the racemic case. It is possible that molecular chirality to some degree destabilizes the 3d layer deformation. However, though, the racemates appear to be more resistant against field effects it was shown in the previous section that birefringent defects were observed in the $DC_{FE}{}^{[*]}$ phases of the racemates whereas the DE_{FE}* phases of the enantiomers are in all cases defect free. This was attributed to the presence of grain boundaries in the $DC_{FE}{}^{[*]}$ phases. These grain boundaries might also have a stabilizing effect on the sponge-like structure of the racemic compound as they allow unfavorable defects, arising from helical deformations, to escape into the defect regions.

As for all other investigated compounds, the polarization peak disappears below a distinct temperature, in this case below 75 °C, due to the increased viscosity in the $DC_{(g)}{}^{[*]}$ and $DE_{(g)}$* phases, respectively.

For the optical investigation of the switching process, compound ***rac*-Si$_3$-3b** was chosen, as for this compound the field-induced layer structure is sufficiently stable also after removing the alignment field. For most other compounds layer deformation arises as soon as 0 V is approached and in these cases the rotation of extinction crosses in circular domains cannot be followed. Circular domains of the field-induced smectic phase of ***rac*-Si$_3$-3b** were grown by slow cooling under a DC field (Fig. 10). The extinction crosses are inclined with polarizer and analyzer indicating a synclinic organization in the field-induced state confirming a strongly tilted organization of the molecules in the DC phases at 0 V as well as in the field-induced states under applied voltage (see Fig. 10).[13,15] A rotation of the extinction crosses is only observed after application of the opposite voltage, which confirms a bistable (ferroelectric) switching and indicates a switching process by rotation on a cone.[13]

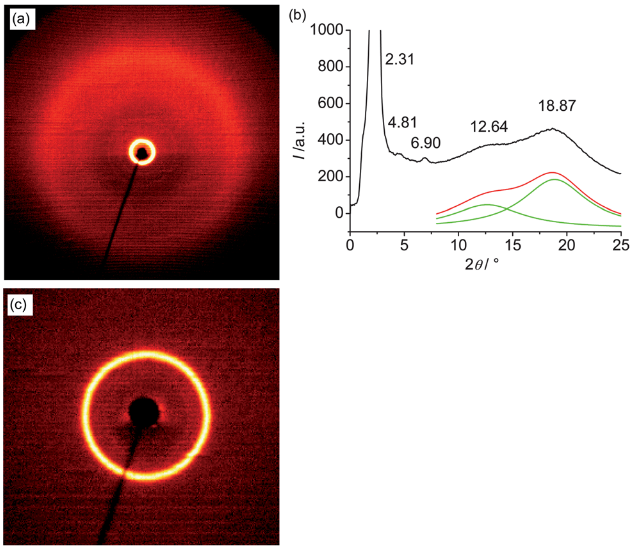

Fig. 6 XRD patterns of the DC$_{\mathrm{FE}}$[*] phase of compound ***rac*-Si$_3$-2a** obtained on a glass substrate (attempted surface alignment) at $T = 110$ °C (a) complete diffraction pattern (bottom is shadowed by the glass substrate) and (b) θ-scan and (c) small angle region showing the completely isotropic distribution of the small angle scattering.

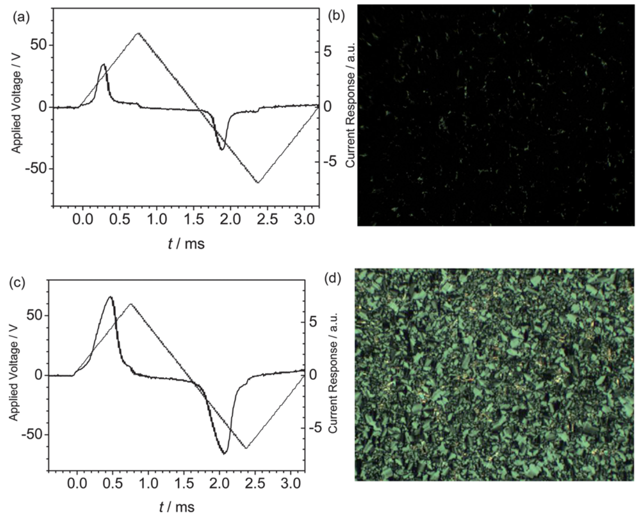

Fig. 8 (a and c) Switching current response obtained for ***rac*-Si$_3$-3b** under a triangular wave field (120 Vpp, 308 Hz, 2 kΩ, 6 μm noncoated ITO cells) and (b and d) the textures observed under these conditions, (a and b) at 141 °C ($P_s = 260$ nC cm^{-2}) and (c and d) at 120 °C ($P_s = 620$ nC cm^{-2}).

2.4.5 Electro-optical investigation of compounds with short chains.

A different behaviour is observed for all compounds with relatively short branched chains (compounds **(*S*)-Si$_3$-1a** and ***rac*-Si$_x$-2a/b**). For these compounds no field-induced formation of a uniform birefringent texture is observed, the appearance of the mesophase remains almost dark even under high field strengths (up to 50 V μm^{-1}), indicating that the layer deformation forces are especially strong in these cases. Only nonspecific small birefringent spots occur in the dark areas of compound **(*S*)-Si$_3$-1a**. This means that for these compounds the sponge-like deformation of the layers is very strong and is retained even under high applied electric fields. For compound **(*S*)-Si$_3$-1a** a single polarization current peak was detected under a relatively high triangular-wave voltage and the spontaneous polarization value (P_s around 330 nC cm^{-2}, see Fig. S5a†) is significantly smaller than those observed for the compounds with the longer chiral chains. For compound ***rac*-Si$_3$-2a** an even smaller single polarization current peak appeared at relatively high voltage (>6 V μm^{-1}) and the spontaneous polarization value is only 3.5 nC cm^{-2} for this compound (Fig. S5b†). No polarization peak is observed for compounds ***rac*-Si$_3$-2b** and ***rac*-Si$_{3i}$-2b** under applied electric fields of up to 50 V μm^{-1}, which for this reason

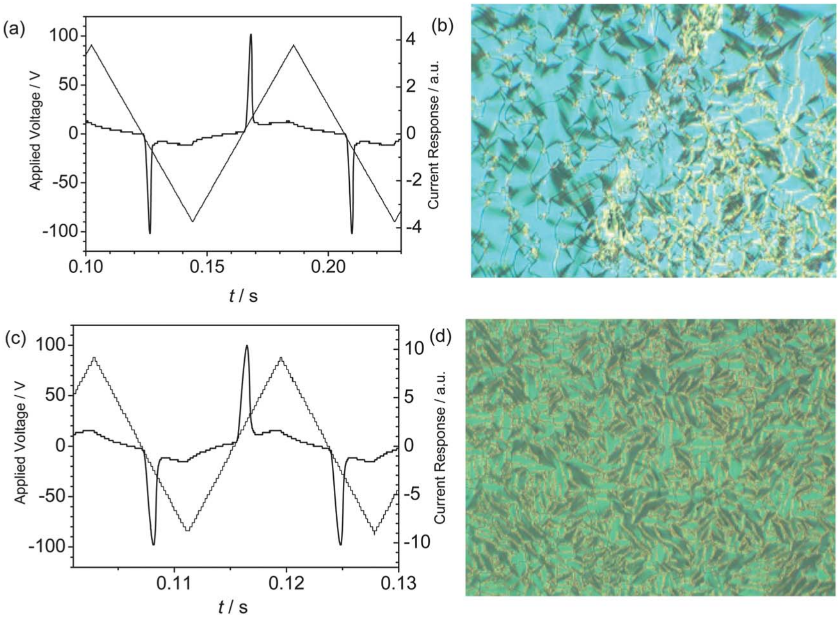

Fig. 7 (a and c) Switching current response obtained under a triangular wave field (6 μm noncoated ITO cells) and (b and d) the corresponding texture of the mesophase of the racemic compounds; (a and b) ***rac*-Si$_{3i}$-3b** (136 °C, 178 Vpp, 12 Hz, 5 kΩ); (c and d) ***rac*-Si$_3$-3a** (131 °C, 170 Vpp, 60 Hz, 5 kΩ).

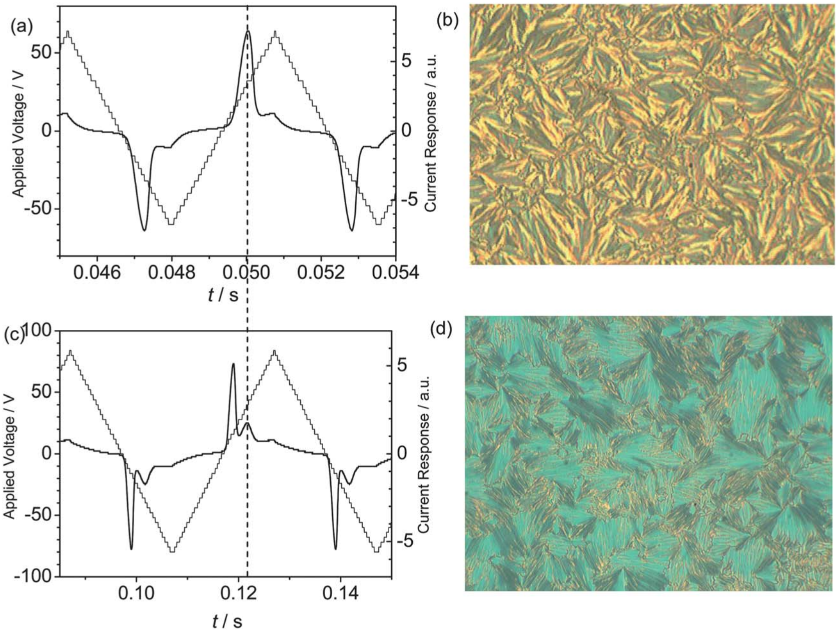

Fig. 9 (a and c) Switching current response obtained for **(*S*)-Si$_3$-3b** in a 6 μm noncoated ITO cell under a triangular wave field and (b and d) the textures observed under these conditions, (a and b) at $T = 120$ °C, 120 Vpp, 180 Hz, 2 kΩ (the same texture is observed at 141 °C, *i.e.* under the same conditions as for the racemate in Fig. 8b) and (c and d) at $T = 125$ °C, 180 Vpp, 25 Hz, 5 kΩ.

are assigned as DC phases, for which no polar switching is observed and no chiral domains can be identified (see Section 2.4.1). The relation between the degrees of field-induced birefringence and measured polarization values confirm that ferroelectric switching is only observed after removal of the sponge-like structure of the dark conglomerate phases. It appears that the relatively short branched group allows an especially strong 3d-layer deformation, giving rise to very stable DE*, DC[*] and DC phases which can be only partly or not removed under strong electric fields.

3. Conclusion

The first examples of chiral polyphilic bent-core molecules with oligo(dimethylsiloxane) end groups have been synthesized in racemic and enantiomerically pure forms. These compounds show dark LC phases with a sponge-like structure similar to the DC[*] phases of related silylated achiral bent-core molecules with linear alkyl chains. In the enantiomers, due to the uniform chirality, these mesophases have uniform optical activity and therefore the darkest state is obtained after decrossing the polarizers by a small angle in a specific direction, defined by the direction of the rotation of the plane of the polarized light. These chiral phases with uniform chirality are assigned as DE* ("dark enantiomer") phases, which represent the homochiral analogues of the dark conglomerate phases (DC[*]).

Under an applied electric field the sponge-like layer deformation in the smectic phases of the enantiomers and racemates can in some, but not in all cases, be removed. If layer deformation is removed, then ferroelectric switching is observed. However, the voltage required to remove the layer deformation is strongly dependent on the molecular structure, and this voltage is regarded as a measure of the strength of layer deformation. It depends mainly on the type of alkyl chain and increases in the order *n*-alkyl < 3,7-dimethyloctyl < 2-methylbutyl < 2-ethylhexyl, *i.e.* it rises the closer the branching point is located to the aromatic core unit and the larger the branch is. Hence, layer distortion increases with the increasing effective average diameter required by the alkyl chains at the aliphatic–aromatic interfaces, which means that steric layer frustration plays an important role in the

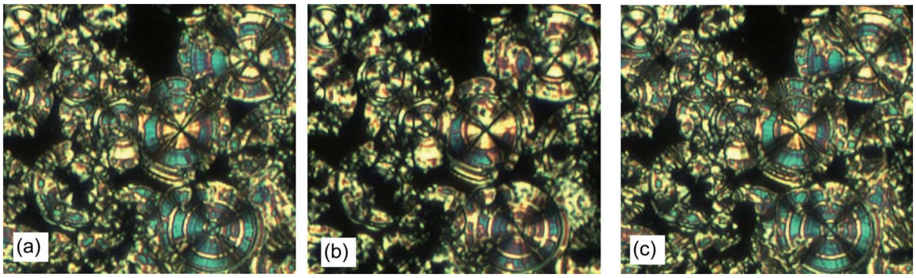

Fig. 10 Optical photomicrographs of circular domains of the DC$_{FE}$[*] phase of compound ***rac*-Si$_3$-3b** at $T = 120$ °C and under a DC voltage of (a) +20 V, (b) 0 V and (c) −20 V, respectively; dark areas represent residues of the DC phase.

formation and stabilization of DC$^{[*]}$, DE* and DC phases. The temperature dependence of the strength of layer distortion is also in line with this assumption, as chain mobility, and hence effective chain diameter increases with rising temperature, requiring a higher voltage to remove layer deformation at higher temperatures. It seems that there is also an effect of chirality on the stability of the sponge structure in the DC$^{[*]}$ and DE* phases. For the enantiomers layer deformation appears to be easier to remove by applying an electric field. It is thought that the grain boundaries, separating the chiral domains in the DC$^{[*]}$ phases, and which are absent in the DE* phases, stabilize the DC$^{[*]}$ structure. The degree of layer deformation (undulation/modulation) remaining in the field-induced smectic phases is influenced by the molecular structure, temperature and electric field strength.

Acknowledgements

H. Ocak is grateful to the Scientific and Technological Research Council of Turkey (TUBITAK) for a research fellowship at Martin Luther University, Halle, Germany. B. Bilgin-Eran is grateful to the Alexander von Humboldt Foundation, for financial support toward liquid crystal research.

References

1 L. Pasteur, *C. R. Acad. Sci.*, 1848, **26**, 535.
2 I. Weissbuch, L. Leiserowitz and M. Lahav, *Top. Curr. Chem.*, 2005, **259**, 123–165.
3 (*a*) A. R. A. Palmans and E. W. Meijer, *Angew. Chem., Int. Ed.*, 2007, **46**, 8948–8968; (*b*) M. M. J. Smulders, I. A. W. Filot, J. M. A. Leenders, P. V. D. Schoot, A. R. A. Palmans, A. P. H. J. Schenning and E. W. Meijer, *J. Am. Chem. Soc.*, 2010, **132**, 611–619.
4 J. A. A. W. Elemans, I. D. Cat, H. Xu and S. D. Feyter, *Chem. Soc. Rev.*, 2009, **38**, 722–736.
5 D. Pijper and B. L. Feringa, *Soft Matter*, 2008, **4**, 1349–1372.
6 V. Percec and P. Leowanawat, *Isr. J. Chem.*, 2011, **51**, 1107–1117.
7 F. Vera, J. L. Serrano and T. Sierra, *Chem. Soc. Rev.*, 2009, **38**, 781–796.
8 Y.-W. Chiang, R.-M. Ho, C. Burger and H. Hasegawa, *Soft Matter*, 2011, **7**, 9797–9803.
9 Y. Snir and R. D. Kamien, *Science*, 2005, **307**, 1067.
10 J. V. Selinger, M. S. Spector and J. M. Schnur, *J. Phys. Chem. B*, 2001, **105**, 7157–7169.
11 H. Nagayama, S. Kumar Varshney, M. Goto, F. Araoka, K. Ishikawa, V. Prasad and H. Takezoe, *Angew. Chem., Int. Ed.*, 2010, **49**, 445–448.
12 H. S. Jeong, S. Tanaka, D. K. Yoon, S.-W. Choi, Y. H. Kim, S. Kawauchi, F. Araoka, H. Takezoe and H.-T. Jung, *J. Am. Chem. Soc.*, 2009, **131**, 15055–15060.
13 (*a*) R. Amaranatha Reddy and C. Tschierske, *J. Mater. Chem.*, 2006, **16**, 907–961; (*b*) H. Takezoe and Y. Takanishi, *Jpn. J. Appl. Phys.*, 2006, **45**, 597–625.
14 T. Niori, T. Sekine, J. Watanabe, T. Furukawa and H. Takezoe, *J. Mater. Chem.*, 1996, **6**, 1231–1233.
15 D. R. Link, G. Natale, R. Shao, J. E. Maclennan, E. Körblova, N. A. Clark and D. M. Walba, *Science*, 1997, **278**, 1924–1927.
16 C. Tschierske, in *Chirality at the Nano Scale*, ed. D. B. Amabiliino, Wiley-VCH, Weinheim, 2009, p. 271.
17 V. Görtz, *Liq. Cryst. Today*, 2010, **19**, 37–48.
18 L. E. Hough, H. T. Jung, D. Krüerke, M. S. Heberling, M. Nakata, C. D. Jones, D. Chen, D. R. Link, J. Zasadzinski, G. Heppke, J. P. Rabe, W. Stocker, E. Körblova, D. M. Walba, M. A. Glaser and N. A. Clark, *Science*, 2009, **325**, 456–460.
19 D. M. Walba, L. Eshdat, E. Körblova and R. K. Shoemaker, *Cryst. Growth Des.*, 2005, **5**, 2091–2099.
20 H.-S. Kitzerow and C. Bahr, *Chirality in Liquid Crystals*, Springer-Verlag, New York, 2001.
21 R. Lemineux, *Chem. Soc. Rev.*, 2007, **36**, 2033–2045.
22 I. Nishiyama, *Chem. Rec.*, 2009, **9**, 340–355.
23 J. W. Goodby, *Curr. Opin. Colloid Interface Sci.*, 2002, **7**, 326–332.
24 (*a*) S. Stojadinovic, A. Adorjan, S. Sprunt, H. Sawade and A. Jakli, *Phys. Rev. E: Stat., Nonlinear, Soft Matter Phys.*, 2002, **66**, 060701; (*b*) D. Wiant, S. Stojadinovic, K. Neupane, S. Sharma, K. Fodor-Csorba, A. Jakli, J. T. Gleeson and S. Sprunt, *Phys. Rev. E: Stat., Nonlinear, Soft Matter Phys.*, 2006, **73**, 030703; (*c*) N. Vaupotic, J. Szydlowska, M. Salamonczyk, A. Kovarova, J. Svoboda, M. Osipov, D. Pociecha and E. Gorecka, *Phys. Rev. E: Stat., Nonlinear, Soft Matter Phys.*, 2009, **80**, 030701(R).
25 K. Kumazawa, M. Nakata, F. Araoka, Y. Takanishi, K. Ishikawa, J. Watanabe and H. Takezoe, *J. Mater. Chem.*, 2004, **14**, 157–164.
26 C. K. Lee, S. S. Kwon, T. S. Kim, E. J. Choi, S. T. Shin, W. C. Zin, D. C. Kim, J. H. Kim and L. C. Chien, *Liq. Cryst.*, 2003, **30**, 1401.
27 S. K. Lee, C. W. Park, J. G. Lee, K. T. Kang, K. Nishida, Y. Shimbo, Y. Takanishi and H. Takezoe, *Liq. Cryst.*, 2005, **32**, 1205.
28 R. A. Reddy, B. K. Sadashiva and U. Baumeister, *J. Mater. Chem.*, 2005, **15**, 3303.
29 M. Nakata, D. R. Link, F. Araoka, J. Thisayukta, Y. Takanishi, K. Ishikawa, J. Watanabe and H. Takezoe, *Liq. Cryst.*, 2001, **28**, 1301–1308.
30 S. K. Lee, S. Heo, J.-G. Lee, K.-T. Kang, K. Kumazawa, K. Nishida, Y. Shimbo, Y. Takanishi, J. Watanabe, T. Doi, T. Takahashi and H. Takezoe, *J. Am. Chem. Soc.*, 2005, **127**, 11085–11091.
31 K. Nishida, M. Cepic, W. J. Kim, S. K. Lee, S. Heo, J. G. Lee, Y. Takanishi, K. Ishikawa, K.-T. Kang, J. Watanabe and H. Takezoe, *Phys. Rev. E: Stat., Nonlinear, Soft Matter Phys.*, 2006, **74**, 021704.
32 H. Ocak, B. Bilgin-Eran, M. Prehm, S. Schymura, J. P. F. Lagerwall and C. Tschierske, *Soft Matter*, 2011, **7**, 8266–8280.
33 (*a*) C. Tschierske, *J. Mater. Chem.*, 1998, **8**, 1485–1508; (*b*) C. Tschierske, *J. Mater. Chem.*, 2001, **11**, 2647–2671; (*c*) F. Tournilhac, L. M. Blinov, J. Simon and S. V. Yablonsky, *Nature*, 1992, **359**, 621–623.
34 (*a*) G. Dantlgraber, A. Eremin, S. Diele, A. Hauser, H. Kresse, G. Pelzl and C. Tschierske, *Angew. Chem., Int. Ed.*, 2002, **41**, 2408–2412; (*b*) G. Dantlgraber, S. Diele and C. Tschierske, *Chem. Commun.*, 2002, 2768; (*c*) C. Tschierske and G. Dantlgraber, *Pramana*, 2003, **61**, 455.
35 R. A. Reddy, U. Baumeister and C. Tschierske, *Chem. Commun.*, 2009, 4236–4238.
36 C. Keith, R. A. Reddy, U. Baumeister and C. Tschierske, *J. Am. Chem. Soc.*, 2004, **126**, 14312–14313.
37 R. A. Reddy, U. Baumeister, C. Keith, H. Hahn, H. Lang and C. Tschierske, *Soft Matter*, 2007, **3**, 558–570.
38 R. Achten, A. Koudijs, M. Giesbers, R. A. Reddy, T. Verhulst, C. Tschierske, A. T. M. Marcelis and E. J. R. Sudhölter, *Liq. Cryst.*, 2006, **33**, 681–688.
39 (*a*) C. Keith, R. A. Reddy, A. Hauser, U. Baumeister and C. Tschierske, *J. Am. Chem. Soc.*, 2006, **128**, 3051–3066; (*b*) C. Keith, R. A. Reddy and C. Tschierske, *Chem. Commun.*, 2005, 871–873; (*c*) C. Keith, G. Dantlgraber, R. A. Reddy, U. Baumeister and C. Tschierske, *Chem.–Eur. J.*, 2007, **13**, 2556–2577; (*d*) Y. Zhang, U. Baumeister, C. Tschierske, M. J. O'Callaghan and C. Walker, *Chem. Mater.*, 2010, **22**, 2869–2884.
40 R. A. Reddy and B. K. Sadashiva, *Liq. Cryst.*, 2003, **30**, 1031.
41 (*a*) W. Weissflog, M. W. Schröder, S. Diele and G. Pelzl, *Adv. Mater.*, 2003, **15**, 630; (*b*) I. Wirth, S. Diele, A. Eremin, G. Pelzl, S. Grande, L. Kovalenko, N. Pancenko and W. Weissflog, *J. Mater. Chem.*, 2001, **11**, 1642.
42 (*a*) J. Thisayukta, Y. Nakayama, S. Kawauchi, H. Takezoe and J. Watanabe, *J. Am. Chem. Soc.*, 2000, **122**, 7441; (*b*) S. K. Lee, L. Shi, M. Tokita, H. Takezoe and J. Watanabe, *J. Phys. Chem. B*, 2007, **111**, 8698–8701; (*c*) S. K. Lee, L. Shi, M. Tokita and J. Watanabe, *J. Phys. Chem. B*, 2008, **112**, 6762–6766.
43 G. Heppke, D. D. Parghi and H. Sawade, *Liq. Cryst.*, 2000, **27**, 313.
44 J. Ortega, C. L. Folcia, J. Etxebarria, N. Gimeno and M. B. Ros, *Phys. Rev. E: Stat., Nonlinear, Soft Matter Phys.*, 2003, **68**, 11707.
45 A. Jakli, Y.-M. Huang, K. Fodor-Csorba, A. Vajda, G. Galli, S. Diele and G. Pelzl, *Adv. Mater.*, 2003, **15**, 1606.
46 (*a*) L. E. Hough, M. Spannuth, M. Nakata, D. A. Coleman, C. D. Jones, G. Dantlgraber, C. Tschierske, J. Watanabe,

E. Körblova, D. M. Walba, J. E. Mclennan, M. A. Glaser and N. A. Clark, *Science*, 2009, **325**, 452; (*b*) D. Chen, Y. Shen, C. Zhu, L. E. Hough, N. Gimeno, M. A. Glaser, J. E. Maclennan, M. Blanca Ros and N. A. Clark, *Soft Matter*, 2011, **7**, 1879–1883.

47 F. Yan, C. A. Hixson and D. J. Earl, *Soft Matter*, 2009, **5**, 4477–4483.

48 S. Kawauchi, S.-W. Choi, K. Fukuda, K. Kishikawa, J. Watanabe and H. Takezoe, *Chem. Lett.*, 2007, **36**(6), 750–751.

49 C. Tschierske and H. Zaschke, *J. Prakt. Chem.*, 1989, **331**, 365–366.

50 (*a*) N. Miyaura, T. Yanagi and A. Suzuki, *Synth. Commun.*, 1981, **11**, 513–519; (*b*) N. Miyaura and A. Suzuki, *Chem. Rev.*, 1995, **95**, 2457–2483; (*c*) M. Hird, G. W. Gray and K. J. Toyne, *Mol. Cryst. Liq. Cryst.*, 1991, **206**, 187–204.

51 (*a*) M. Xie, J. Qin, Z. Hu and H. Zhao, *Chin. Chem. Lett.*, 1992, **3**, 775–778; (*b*) Q. Jun, X. Ming-Gui, H. Zi-Lun, Z. Hua-Ming and L. Shi-Kui, *Synth. Commun.*, 1992, **22**, 2253–2258.

52 R. Achten, A. Koudijs, M. Giesbers, A. T. M. Marcelis and E. J. R. Sudhölter, *Liq. Cryst.*, 2005, **32**, 277.

53 B. Schiewe, A. Hohmuth, W. Weissflog and H. Kresse, *Mol. Cryst. Liq. Cryst.*, 1996, **287**, 115–127.

54 B. Otterholm, M. Nilsson, S. T. Lagerwall and K. Skarp, *Liq. Cryst.*, 1987, **2**, 757–769.

55 G. H. Mehl and J. W. Goodby, *Chem. Ber.*, 1996, **129**, 521–525.

56 S. Kang, M. Tokita, Y. Takanishi, H. Takezoe and J. Watanabe, *Phys. Rev. E: Stat., Nonlinear, Soft Matter Phys.*, 2007, **76**, 042701.

57 H. Hahn, C. Keith, H. Lang, R. A. Reddy and C. Tschierske, *Adv. Mater.*, 2006, **18**, 2629–2633.

Addition and correction

Note from RSC Publishing

This article was originally published with incorrect page numbers. This is the corrected, final version.

The Royal Society of Chemistry apologises for these errors and any consequent inconvenience to authors and readers.